Author Manuscript

Author Manuscript

Author Manuscript

Author Manuscript

HHS Public Access

Author manuscript

J Biomed Mater Res B Appl Biomater. Author manuscript; available in PMC 2019 December 27.

Published in final edited form as:

J Biomed Mater Res B Appl Biomater. 2019 August ; 107(6): 2019–2029. doi:10.1002/jbm.b.34293.

Toward zonally tailored scaffolds for osteochondral differentiation of synovial mesenchymal stem cells

Patricia Diaz-Rodriguez[1], **Josh D. Erndt-Marino**[1,†], **Tanmay Gharat**[2,†], **Dany J. Munoz Pinto**[1], **Satyavrata Samavedi**[1], **Robert Bearden**[3], **Melissa A. Grunlan**[4], **W. Brian Saunders**[3], **Mariah S. Hahn**[2]

[1]Department of Biomedical Engineering, Rensselaer Polytechnic Institute, Troy, New York

[2]Department of Chemical and Biological Engineering, Rensselaer Polytechnic Institute, Troy, New York

[3]Veterinary Medicine and Biomedical Sciences, Texas A&M University, College Station, Texas

[4]Department of Biomedical Engineering, Texas A&M University, College Station, Texas

Abstract

Synovium-derived mesenchymal stem cells (SMSCs) are an emerging cell source for regenerative medicine applications, including osteochondral defect (OCD) repair. However, in contrast to bone marrow MSCs, scaffold compositions which promote SMSC chondrogenesis/osteogenesis are still being identified. In the present manuscript, we examine poly(ethylene) glycol (PEG)-based scaffolds containing zonally-specific biochemical cues to guide SMSC osteochondral differentiation. Specifically, SMSCs were encapsulated in PEG-based scaffolds incorporating glycosaminoglycans (hyaluronan or chondroitin-6-sulfate [CSC]), low-dose of chondrogenic and osteogenic growth factors (TGFβ1 and BMP2, respectively), or osteoinductive poly(dimethylsiloxane) (PDMS). Initial studies suggested that PEG-CSC-TGFβ1 scaffolds promoted enhanced SMSC chondrogenic differentiation, as assessed by significant increases in Sox9 and aggrecan. Conversely, PEG-PDMS-BMP2 scaffolds stimulated increased levels of osteoblastic markers with significant mineral deposition. A "Transition" zone formulation was then developed containing a graded mixture of the chondrogenic and osteogenic signals present in the PEG-CSC-TGFβ1 and PEG-PDMS-BMP2 constructs. SMSCs within the "Transition" formulation displayed a phenotypic profile similar to hypertrophic chondrocytes, with the highest expression of collagen X, intermediate levels of osteopontin, and mineralization levels equivalent to "bone" formulations. Overall, these results suggest that a graded transition from PEG-CSC-TGFβ1 to PEG-PDMS-BMP2 scaffolds elicits a gradual SMSC phenotypic shift from chondrocyte to hypertrophic chondrocyte to osteoblast-like. As such, further development of these scaffold formulations for use in SMSC-based OCD repair is warranted.

Correspondence to: M. S. Hahn; hahnm@rpi.edu.
†These authors contributed equally to this work.

Additional Supporting Information may be found in the online version of this article.

Author Manuscript Author Manuscript Author Manuscript Author Manuscript

Keywords

chondrogenesis; osteochondral tissue; osteogenesis; PEG scaffolds; synovium-derived mesenchymal stem cells

INTRODUCTION

Osteochondral defects (OCDs) are localized damage of cartilage and underlying subchondral bone, which can cause pain and loss of joint function.[1–5] Due to the poor intrinsic healing potential of cartilage and the associated deterioration of the exposed subchondral bone, untreated OCDs progressively worsen and may result in degenerative diseases such as osteoarthritis.[3–5] Current clinical treatments require further tissue damage in order to achieve therapeutic effects[2,6] or the use of allografts with their concomitant risks of disease transmission and immune rejection.[7] Considering these limitations, tissue engineering approaches could represent a promising alternative for OCD repair and regeneration. However, the unique and complex structure (which gives rise to function) of the osteochondral unit and interface has proven challenging to reconstruct, hampering clinical success. In particular, the osteochondral interface is critical to ensuring a gradual, non-stress concentrating transfer of load from cartilage to bone.[8] While the osteochondral unit is continuous, it generally consists of three distinct tissue regions—cartilage, calcified cartilage, and the underlying calcified subchondral bone—each with distinct extracellular matrix (ECM) composition and cell types.[9] Thus, an ideal tissue engineered scaffold should stimulate associated cells to recapitulate the zonally-specific structure and function of the osteochondral unit.

Conventionally, tissue engineering approaches are comprised of a biomaterial scaffold to provide a three-dimensional (3D) architecture combined with cells and bioactive stimuli (e.g., growth factors or material-mediated cues) to induce desired cell responses.[10] Due to their capacity to acquire both chondrocyte-like and osteoblast-like phenotypes, mesenchymal stem cells (MSCs) harvested from bone marrow have been a common cell source for tissue engineering approaches for OCD repair. However, the painful harvesting procedure and low MSC yields obtained per biopsy have led researchers to investigate alternate MSC sources, including the synovium surrounding the joint.[11,12]

Since their isolation and characterization in 2001,[13] many studies have pointed out the advantages synovium-derived MSCs (SMSCs). In particular, SMSCs can be extracted at 60 to 100-fold higher yields per nucleated cell relative to bone marrow MSCs,[14,15] and the harvesting procedure is relatively noninvasive and is associated with minimal complications at the donor site.[13,15] Moreover, it has been reported that SMSCs possess a high degree of multipotency, remaining unaffected by donor age, cell passages up to passage 10, and cryopreservation.[13,16] These advantages make SMSCs a promising cell source for osteochondral regeneration. While methods to guide SMSC chondrogenic and osteogenic differentiation have been studied previously,[14,15,17–20] these approaches often implement high dosages of growth factors such as transforming growth factor-β1 (TGFβ1) and bone morphogenic protein 2 (BMP2), which are associated with high costs and negative side

Author Manuscript Author Manuscript Author Manuscript Author Manuscript

effects.[21–23] In addition, although bone marrow MSC responses to a range of scaffold-based biochemical stimuli have been systematically examined, SMSC responses to 3D scaffold formulations are just beginning to be understood and characterized. For example, a majority of the work with SMSCs has focused on chondrogenic applications with scaffold-free approaches[24,25] or using a variety of different scaffolds, including collagen[26] and gelatin-dextran.[27] However, studies which allow comparison of SMSC differentiation in response to defined scaffold-based biochemical signals are limited,[28] as are reports of scaffold-based SMSC osteogenic differentiation.[29,30] This situation hampers efforts to improve the design of scaffolds intended to drive the chondrogenic and osteogenic SMSC differentiation needed for tissue engineered osteochondral applications.

In the present work, we seek to identify specific, scaffold-based biochemical cues which stimulate SMSC differentiation into the functional cell types within the osteochondral unit (i.e., chondrocytes, hypertrophic chondrocytes, and osteoblasts). To ensure defined presentation of desired biochemical signals, poly(ethylene glycol) (PEG)-based scaffolds will be utilized. Photo-polymerizable PEG-based scaffolds offer a versatile platform for fabricating scaffolds with the spatially varying properties needed for OCD repair via 3D printing,[31,32] gradient,[33–35] or stereolithographic[36] methods. Furthermore, PEG-based scaffolds are intrinsically resistant to serum protein adsorption, cell attachment, and spreading.[37] This biological "blank slate" character permits the controlled presentation of desired biochemical cues (e.g., ECM components[38,39] and growth factors[40,41]) and systematic examination of their effects on cell behavior. Moreover, growth factors tethered into PEG-based scaffolds are effectively inhibited from being internalized by cells,[40,42] allowing for repeated signaling by a single growth factor molecule and use of lower growth factor doses.[43,44]

With the beneficial properties of PEG-systems and their prior use in cartilage[45–50] and bone[41,51–53] applications in mind, the overall goal of this work is to develop a set of PEG-based scaffolds—each presenting a defined combination of biochemical cues and low-dose growth factors—to enable the zonally-specific SMSC differentiation needed for OCD repair. In selecting biochemical signals to analyze, we focused on cues that have been shown to support bone marrow MSC chondrogenesis or osteogenesis so as to identify potential similarities in SMSC and bone marrow MSC responses. In particular, PEG-based scaffolds incorporating TGFβ1[54,55] or hyaluronan (HA)[56,57]/chondroitin sulfate (CS)[39,58]—two glycosaminoglycans (GAGs) abundant in cartilage—have been shown to promote chondrocyte-specific phenotypic signatures. Similarly, PEG-scaffolds incorporating hydrophobic, inorganic poly(dimethylsiloxane) (PDMS) along with low-dose BMP2 stimulate bone marrow MSC osteoblastic differentiation while maintaining a non-brittle, elastomeric structure for physiological loading.[43,59]

In the current work we therefore focused on varying the levels of PDMS, tethered BMP2, tethered TGFβ1, and incorporated HA or chondroitin-6-sulfate (CSC) within PEG-based scaffolds to promote zonally-specific SMSC differentiation into cellular phenotypes consistent with the cartilage, transition, and bone regions of the osteochondral unit. Through a series of initial "tuning" experiments, we identified "Cartilage" and "Bone" scaffold formulations that induced specific chondrogenic and osteogenic differentiation, respectively.

Author Manuscript Author Manuscript Author Manuscript Author Manuscript

We then developed a "Transition" zone/interface scaffold formulation, after which we confirmed that our zonal formulations stimulated SMSCs to recapitulate the graded phenotypic profiles representative of the osteochondral unit.

MATERIALS AND METHODS

Preparation of diacrylate-terminated PEG and methacrylate-terminated star PDMS

Diacrylate-terminated PEG (PEGDA, M_n = 3.4 kDa) and methacrylate-terminated star PDMS ($PDMS_{star}$-MA, M_n = 2 kDa) were prepared accordingly to previously described protocols.[59–62] $PDMS_{star}$-MA methacrylation was confirmed by proton nuclear magnetic resonance (^{1}H-NMR) to be >90%. Acrylation of the PEG end hydroxyl groups was also characterized by ^{1}H-NMR to be ~97.5%. At this PEG acrylation level, 92%–100% incorporation of methacrylated HA/CSC, acrylate-derivatized RGDS, and acrylate-derivatized growth factors is achieved using the photopolymerization conditions used herein.[44,63,64]

Preparation of methacrylated HA and CSC

HA and CSC were selected for evaluation based on their structural role in cartilage, their chondroprotective effects, and their ability to facilitate chondrogenesis.[39,65–70] In order to conjugate these GAGs into the PEGDA-based scaffolds, each GAG type was methacrylate-derivatized according to standard protocols.[71] In brief, CSC (51 kDa, 6.4 wt % sulfur, Sigma) and HA (*Streptococcus equi*, M_W ~ 1.65×10^3 kDa, Fluka) were dissolved in deionized (dI)H_2O to achieve a 1 wt % final concentration, and the pH of each solution was adjusted to 8.0. A 10-fold molar excess of methacrylic anhydride (Polysciences) was added per disaccharide unit, and each reaction was allowed to proceed under constant stirring at 4°C at pH ~ 8.0. The product of each reaction was precipitated twice using chilled 95% ethanol, dialyzed against dIH_2O for 48 hr, and lyophilized. The extent of methacrylate-derivatization of both CSC-MA and HA-MA was characterized by ^{1}H-NMR to be ~1.0%–1.6%. (per available −OH groups). These levels of methacrylate-derivatization have previously been shown to negligibly alter observed cell-GAG interactions[38] yet to be sufficient to avoid significant sol in PEGDA networks.[64]

Methacrylated HA of intermediate molecular weight (HA_{IMW}-MA) was subsequently prepared according to previously described protocols.[38,64,72] In brief, HA-MA was dissolved at 1 mg/ml in phosphate buffered saline (PBS) containing 5 U/ml hyaluronidase IV-S (H3884, Sigma). Following 12 hr treatment overnight at 37°C, the enzyme was heat-inactivated. The resulting digestion product was dialyzed against dIH_2O for 48 hr and lyophilized. The average molecular weight of the isolated HA_{IMW}-MA was determined to be ~600 kDa, with a polydispersity of ~1.3, using gel permeation chromatography (Viscotek). This average molecular weight is within the range noted for chondroprotective effects.[73]

Synthesis of acrylate-derivatized peptides and growth factors (RGDS, BMP2, and TGFβ1)

Addition of acryl groups to RGDS (American Peptide), human recombinant carrier free BMP2 (R&D systems), and human recombinant carrier free TGFβ1 (EMD Millipore) was carried out via reaction with acryloyl-PEG-succinimidyl valerate (ACRL-PEG-SVA, 3.4

Author Manuscript Author Manuscript Author Manuscript Author Manuscript

kDa; Laysan Bio) at a 1:1 molar ratio for RGDS or 1:6 molar ratio for BMP2 and TGFβ1. Reconstituted TGFβ1 and BMP2 were first dialyzed to non-growth factor associated primary amines. The resulting mixtures were reacted for 2 hr in 50 m*M* sodium bicarbonate buffer, pH 8.5.[74,75] The ACRL-PEG-RGDS was purified by dialysis overnight against dIH_2O at 4°C using 3500 MWCO Snakeskin Dialysis tubing (Thermo Fisher Scientific) to remove unreacted ACRL-PEG-SVA. ACRL-PEG-BMP2 and ACRL-PEGTGFβ1 were purified by dialysis overnight against dIH_2O at 4°C using 5000 MWCO Snakeskin Dialysis tubing.

Tissue collection and cell isolation

Canine SMSC isolation was conducted with the approval of the Texas A&M University Institutional Animal Care and Use Committee (Animal Use Protocol 2015–0072). SMSCs were isolated using previously described techniques.[14] Briefly, canine synovium samples were obtained during knee arthroscopy and surgery for cranial cruciate ligament rupture. Under general anesthesia, a synovium/subsynovial biopsy was isolated from the proximolateral femoropatellar joint using arthroscopic biopsy forceps. Primary SMSCs were isolated from three donors to partially control for age and breed effects: (1) a 1.2-year-old, 65 lb intact male Walker hound (~equivalent to a 16.5-year-old human), (2) a 6-yearold, 148 lb neutered male mixed breed (~equivalent to a 46–49-year-old human), and (3) a 3.5-year-old, 47 lb neutered male mixed breed (~equivalent to a 30-year-old human).

As expected,[14] SMSCs at passage 1 were negative for CD34 and CD45 and positive for CD9, CD44, CD90, CD105, and STRO-1 (Supporting Information Figure S1). Isolated SMSCs were also confirmed to be able to differentiate down adipogenic, chondrogenic, and osteogenic lineages by standard methodologies (Supporting Information Figure S1). Characterization at passage 1 is considered a standard as long as appropriate culture conditions (e.g., <70% confluence) are maintained, and SMSCs have been shown to maintain stable surface antigen expression through passages 4–7.[13] The cells in the present study were utilized at passage 3.

Fabrication of cell-laden constructs

In each study, PEGDA and ACRL-PEG-RGDS were combined with $PDMS_{star}$-MA, HA_{IMW}-MA, CSC-MA, ACRL-PEG-TGFβ1, and/or ACRL-PEG-BMP2 to yield scaffold formulations intended to stimulate desired differentiation.

Initial chondrogenic and osteogenic scaffold formulation assessment.—As an initial assessment of various biochemical moieties on SMSC chondrogenic and osteogenic differentiation, 10 wt % PEGDA solutions containing: (1) 5 mg/ml HA_{IMW}-MA, 5 ng/ml TGFβ1, and 1 m*M* RGDS (“Cartilage”), (2) 4 wt % $PDMS_{star}$-MA, 5 ng/ml BMP2, and 1 m*M* RGDS (“Bone”), or (3) and 1 m*M* RGDS (“PEG” control) were prepared in PBS.

The concentration for the GAG component of our “Cartilage” formulation was selected to be consistent with the upper range of the total GAG content of normal (non-diseased) hyaline cartilage (0.022–0.055 mg/mg dry weight).[76] For reference, 1 ml of a 10 wt % PEGDA hydrogel has a dry weight of 100 mg. In terms of the “Bone” constructs, previous work has demonstrated that 100–500 ng/ml of tethered BMP2 can be as potent as higher doses of

Author Manuscript Author Manuscript Author Manuscript Author Manuscript

soluble BMP2 in driving osteogenic differentiation.[43,77–80] In the present article, we utilized a tethered BMP2 concentration of 50 ng/ml due to internal data demonstrating that 50 ng/ml of tethered BMP2 supported SMSC osteogenic differentiation to a similar extent as 100 ng/ml of tethered BMP2 while reducing undesired chondrogenic marker expression (Supporting Information Figure S2). Furthermore, PDMS was increased to 4 wt % from the 2 wt % utilized in previous bone marrow MSC studies based upon the increased osteopontin (OPN) production and mineralization associated with PDMS incorporation.[43]

Tuning "cartilage" scaffold composition to enhance chondrogenesis.— Following mono-culture and co-culture assessment of the above chondrogenic and osteogenic formulations, we evaluated the effect of replacing HA_{IMW} with CSC on the chondrogenic differentiation of SMSCs. For this study, cells were encapsulated in 10 wt % PEGDA solutions containing:

1. 5 mg/ml HA_{IMW}-MA, 5 ng/ml TGFβ1, and 1 m*M* RGDS or
2. 5 mg/ml CSC-MA, 5 ng/ml TGFβ1, and 1 m*M* RGDS.

Assessment of a "transition" formulation relative to "cartilage" and "bone" scaffolds.—To assess our capacity to induce SMSC differentiation appropriate to each zone of the osteochondral unit, SMSCs were encapsulated in 10 wt % PEGDA solutions containing: (1) 5 mg/ml CSC-MA, 5 ng/ml TGFβ1, and 1 m*M* RGDS ("Cartilage"), (2) 0.5 wt % $PDMS_{star}$-MA, 2 ng/ml TGFβ1, 20 ng/ml BMP2, and 1 m*M* RGDS ("Transition"), or (3) 4 wt % $PDMS_{star}$-MA, 50 ng/ml BMP2, and 1 m*M* RGDS ("Bone").

In all studies, passage 3 SMSCs expanded in αMEM containing 10% fetal bovine serum (FBS; Atlanta Biologics Premium Select) and 1% PSG (Penicillin–Streptomycin–Glutamine, Cell-Gro) were collected and resuspended on the polymer precursor solutions to yield a post-swelling cell density of 1.5×10^6 cells/ml scaffold. Photoinitiator (a 30 wt % solution of 2,2-dimethyl-2-phenyl-acetophenone in N-vinylpyrrolidone) was added to each precursor solution at a concentration of 10 μl/ml. The precursor solutions were then pipetted into separate rectangular molds with 0.75 mm spacers and polymerized by 6 min exposure to long-wave UV light (~6 mW/cm^2, 365 nm). Hydrogels slabs were rinsed with sterile PBS (pH 7.4; Invitrogen), and a sterile biopsy punch was used to process each slab into a series of 8 mm discs. These discs were cultured in Dulbecco's modified Eagle's medium supplemented with 10% FBS and 1% PS at 37°C/5% CO_2 for 21 days, with medium changes every 2 days. For co-culture studies, cell-laden scaffold discs were placed into 24-well plates separated by a Transwell insert. "Cartilage" and "Bone" discs were cultured in the upper and lower compartments, respectively.

Construct collection and analyses

Following 24 hr of swelling, a set of "day 0" discs (n = 4–6 per formulation) were collected for mechanical characterization. After 21 days of culture, additional constructs (n = 4–8 per formulation per assay) were collected for endpoint mechanical, western blot, and histological analyses. Samples for Western blot assessments were snap-frozen and stored at

Author Manuscript Author Manuscript Author Manuscript Author Manuscript

−80°C until use, while samples for histological assays were fixed in formalin and embedded in OCT medium (TissueTek).

Mechanical characterization.—The diameter and thickness of each disc collected for mechanical assessment was measured using a digital micrometer. Following application of a 0.01 N preload, each disc was subjected to unconstrained compression at a strain rate of 1 mm/min using an Instron 3342. The compressive modulus of each hydrogel formulation was extracted from the resulting stress–strain data over a strain range of 0%–10%. As anticipated for constructs compositionally dominated by PEGDA, the "day 0" compressive modulus for all formulations examined measured at ~280 kPa (Supplementary Table S1). In addition, due to the tight crosslink density and the slow degradation rate of PEGDA scaffolds[81–84], the "day 21" compressive modulus was also ~280 kPa for all formulations (Supporting Information Table S1).

Western blot analysis.—Samples for protein analyses were homogenized in lysis buffer (Ambion, Life Technologies), and the supernatant was collected following centrifugation. DNA levels in the supernatant solutions were then measured using the PicoGreen assay (Invitrogen), with calf thymus DNA (Sigma) serving as a standard. Homogenates were concentrated using 3000 MWCO Amicon filter units (Millipore), followed by addition of β-mercaptoethanol and heating at 95°C for 10 min. Concentrated protein samples with consistent DNA levels were loaded into different wells of 8% or 12% polyacrylamide gels and separated by electrophoresis. Proteins were transferred to a nitrocellulose membrane, and primary antibodies for Sox9, osterix (Osx), Collagen II (Col II), tissue non-specific alkaline phosphatase (TNAP), or β-actin (Supporting Information Table S2) were applied overnight at 4°C with constant shaking, as previously described.[85]

Bound primary antibodies were detected by the application of appropriate horseradish peroxidase-conjugated or alkaline phosphatase (AP)-conjugated secondary antibodies (Jackson ImmunoResearch), followed by the application of Luminol (Santa Cruz Biotechnology) or Novex chemiluminescent substrate (Life Technologies) respectively. Chemiluminescence was detected using a ChemiDoc XRS$^+$ System equipped with Image Lab Software (BioRad), with exposure time controlled to avoid signal saturation. The band integrated optical density for each marker was quantified using Adobe Photoshop and normalized to β-actin.

Immunohistochemical analysis.—Embedded histological samples were cryosectioned at 20 μm thickness, after which relative protein levels of OPN, Collagen X (Col X), and aggrecan were assessed using standard immunohistochemical techniques (Supporting Information Table S2). In brief, rehydrated sections were blocked for 10 min by exposure to Terminator solution (Biocare Medical). Samples were incubated at 4°C overnight with primary antibody diluted in PBST (PBS plus 0.1% Tween 20) containing 3% bovine serum albumin. Bound primary antibody was detected using the appropriate AP-conjugated secondary antibody (Jackson Immunoresearch) followed by the application of chromogen Ferangi Blue (Biocare Medical) and mounting. Stained sections were imaged using a Zeiss Axiovert microscope.

Author Manuscript Author Manuscript Author Manuscript Author Manuscript

von Kossa staining.—von Kossa staining was used to assess mineralization according to the manufacturer's protocol (American Mastertech Scientific). Rehydrated sections were rinsed with water, after which a 5% silver nitrate solution was applied, followed by 1 hr exposure to full-spectrum light. Samples were then rinsed with distilled (d)H_2O, exposed to 5% sodium thiosulfate for 3 min, briefly rinsed with dH_2O, and mounted. Stained sections were imaged using a Zeiss Axiovert microscope.

Semi-quantitative staining assessment.—It should be noted that matrix deposition confined to the immediate pericellular space is standard for the PEG-based scaffolds and time frames used herein due to their tight nanoscale mesh structure and slow *in vitro* degradation rate.[81–84] Thus, cell counts were carried out to semi-quantitatively evaluate immunostaining and von Kossa staining according to established methods.[86–88] Each cell, i, in a given section was assigned a staining intensity, d_i, on a scale of 0–3 (0 = "no staining" and 3 = "highest intensity among all formulations for that antibody"). The cumulative staining intensity, d, for a given antibody in a particular section was then calculated using the following equation: $d = (\sum d_i)/(\text{total cell number})$. A minimum of eight sections per sample per treatment group were assessed.

Statistical analyses

All data are reported as the mean ± standard error of the mean. After testing the homogeneity of variance assumption using Levene's test, comparison of experimental group means (n = 4–8 samples per experimental group) was performed by a Tukey's post-hoc test or by a Games-Howell post-hoc test in cases where Levene's test returned a significant result. For all tests, a p-value <.05 was considered significant and SPSS software was utilized.

RESULTS

Initial chondrogenic and osteogenic scaffold formulation assessment

To gain initial insight into the effects of various biochemical moieties on SMSC chondrogenic and osteogenic differentiation, SMSC responses to "Cartilage" constructs (PEG-HA_{IMW}-TGFβ1) and "Bone" constructs (PEG-PDMS-BMP2) were evaluated following 21 days of culture. Specifically, the levels of chondrogenic markers Sox9 and Col II and osteogenic markers TNAP, OPN, and mineralization were assessed relative to "PEG" controls (Figure 1). Representative western blot and immunostaining images are shown in Supporting Information Figure S3.

Although levels of the chondrogenic transcription factor Sox9 remained unchanged in the "Cartilage" constructs relative to "PEG" controls, the presence of HA_{IMW} and TGFβ1 promoted a significant increase in the deposition of Col II (~1.9-fold, $p = .025$). Furthermore, "Cartilage" constructs displayed a marked decrease in mineralization (~3.0-fold, $p = .015$; Figure 1) relative to "PEG" scaffolds, despite a significant increase in TNAP levels relative to "PEG" controls (~2.0-fold, $p < .0005$). Conversely, the presence of 4 wt % $PDMS_{star}$ and 50 ng/ml BMP2 supported a significant increase in all osteogenic markers analyzed (TNAP, OPN, and mineralization; > 2.2-fold, $p < .0005$) but no change in

Author Manuscript Author Manuscript Author Manuscript Author Manuscript

chondrogenic markers Sox9 and Col II relative to "PEG" controls. Cumulatively, these results indicate two main points: (1) the combination of HA_{IMW} and TGFβ1 promoted chondrogenic differentiation but incompletely suppressed osteogenic differentiation and (2) the combination of $PDMS_{star}$ and BMP2 induced a strong and specific osteogenic response.

Co-culture assessment of initial "cartilage" and "bone" formulations

Since crosstalk between the cartilage and bone regions of the osteochondral unit is known to occur *in vivo* and can impact zonal cell phenotype,[89] we reasoned that the incomplete suppression of osteogenic differentiation within the "Cartilage" constructs may be improved through co-culture with the "Bone" constructs. Moreover, it was also important to evaluate possible detrimental effects of co-culture on observed SMSC responses. In terms of the "Cartilage" constructs, 21 day co-culture with "Bone" scaffolds elicited not only a significant decrease in Sox9 (~1.3-fold, $p = .017$) but also a significant increase in OPN (~3.0-fold, $p = .001$) relative to mono-culture "Cartilage" constructs (Figure 2). In contrast, co-culture had a minimal impact on the expression of chondrogenic and osteogenic markers in the "Bone" constructs (Figure 3). Cumulatively, these data suggested an overall osteogenic effect of co-culture and emphasized a need for an alternative "Cartilage" scaffold formulation.

As we expanded our studies to investigate alternative chondrogenic approaches, we simultaneously assessed variability in outcomes with SMSC donor (n = 3) utilizing our "PEG" and "Bone" scaffolds. Importantly, similar SMSC responses persisted across donors of differing ages and neuter status (Supporting Information Figure S4).

Tuning "cartilage" scaffold composition to enhance chondrogenesis

In order to improve SMSC chondrogenic differentiation in the "Cartilage" constructs, the composition of the scaffolds was modified by replacing HA_{IMW} with an equivalent wt % of CSC, while retaining the TGFβ1 concentration at 5 ng/ml. Following 21 days of culture, assessment of chondrogenic and osteogenic markers was performed (Figure 4). PEG-CSC-TGFβ1 scaffolds exhibited significantly increased levels of chondrogenic markers Sox9 (~1.5-fold, $p = .010$) and aggrecan [~4.6-fold, $p < .0005$; Figure 4(A)] but unchanged levels of Col II relative to PEG-HA_{IMW}-TGFβ1 constructs. In addition, PEG-CSC-TGFβ1 constructs were associated with a significant decrease in TNAP levels [~2.0-fold, $p < .0005$; Figure 4(B)] and no change in OPN relative to PEG-HA_{IMW}-TGFβ1 constructs. Cumulatively these data suggest that incorporation of CSC in place of HA_{IMW} was able to enhance both the degree and specificity of SMSC chondrogenic differentiation.

Assessment of a "transition" formulation relative to "cartilage" and "bone" scaffolds

After confirming that CSC resulted in improved chondrogenic behavior in our PEG-based "Cartilage" constructs, a "Transition" scaffold formulation was fabricated to contain a graded mixture of the chondrogenic and osteogenic signals utilized in the PEG-CSC-TGFβ1 "Cartilage" constructs and the PEG-PDMS-BMP2 "Bone" constructs. This "Transition" scaffold—a 10 wt % PEGDA scaffold containing 0.5 wt % $PDMS_{star}$-MA, 2 ng/ml TGFβ1, 20 ng/ml BMP2, and 1 m*M* RGDS—was designed to induce SMSC differentiation into hypertropic chondrocytes. CSC-MA was not included in "Transition" scaffold due to

Author Manuscript Author Manuscript Author Manuscript Author Manuscript

previous work suggesting that CSC is a potent inhibitor of hypertrophic chondrocyte differentiation.[39,90] The effects of the "Cartilage," "Transition," and "Bone" constructs on SMSCs were then compared.

SMSCs cultured in the "Cartilage" constructs generally expressed the highest levels of chondrogenic markers Sox9 and Col II, although the only significant difference noted was between "Cartilage" and "Bone" for Sox9 (~2.0-fold, $p < .0005$; Figure 5). In contrast, "Cartilage" constructs produced significantly lower levels of the hypertrophic chondrocytic marker Col X relative to both "Transition" (~2.2-fold, $p < .0005$) and "Bone" constructs (~1.7-fold, $p = .011$), with the "Transition" scaffolds being associated with the highest levels of Col X ($p < .0005$). The "Transition" scaffolds also produced a higher Osx/Sox9 ratio, another metric of hypertrophic chondrocytic differentiation,[91–93] relative to "Cartilage" constructs (~1.8-fold, $p = .026$).

SMSCs also displayed a general increase in osteogenic markers from 'Cartilage' to "Transition" to "Bone". Specifically, cells cultured in "Cartilage" scaffolds produced significantly lower levels of the osteogenic marker OPN relative to "Transition" (~3.7-fold, $p < .0005$) and "Bone" (~7.6-fold, $p < .0005$) constructs in addition to significantly lower levels of mineralization relative to both "Transition" and "Bone" scaffolds (>2.7-fold, $p < .0005$; (Figure 5). Moreover, the levels of TNAP and OPN were both significantly greater in "Bone" constructs relative to both "Cartilage" (>2.4-fold, $p \leq .002$) and "Transition" (>1.5-fold, $p \leq .032$) scaffolds. Representative Western blot and immunostaining images are provided in Supporting Information Figure S5.

Cumulatively, these data suggest that the formulations tested herein are capable of inducing SMSC phenotypic differentiation consistent with osteochondral tissue (from chondrocyte to hypertrophic chondrocyte to osteoblast), at least in mono-culture. The maintenance of this graded phenotypic transition in a tri-culture scenario will however need to be confirmed prior to preclinical assessments.

DISCUSSION

SMSCs are an emerging cell source for regenerative medicine applications, including for bone[29,30] and cartilage[24–27] applications. The long-term goal of this work was to identify scaffold-based biochemical cues capable of guiding zonally-tailored SMSC differentiation for OCD repair.[94,95] However, in contrast to bone marrow MSCs, scaffold compositions which promote SMSC chondrogenesis/osteogenesis are still being identified. In the present work, we evaluated the effects of a subset of biochemical cues using PEG-based scaffolds. Specifically, SMSCs were encapsulated in PEG-based scaffolds presenting varying combinations of TGFβ1, BMP2, PDMS, and HA_{IMW} or CSC to promote zonally-specific SMSC differentiation into cellular phenotypes consistent with the cartilage, transition, and bone regions of the osteochondral unit.

We began our studies by assessing the capacity of initial "Cartilage" (PEG-HA_{IMW}-TGFβ1) and "Bone" (PEG-PDMS-BMP2) formulations to induce specific SMSC chondrogenic and osteogenic differentiation, respectively. This pilot study revealed that, relative to "PEG"

Author Manuscript Author Manuscript Author Manuscript Author Manuscript

controls, PEG-HA_{IMW}-TGFβ1 scaffolds induced SMSC chondrogenic differentiation (↑Col II, ↓mineralization), but this differentiation appeared to be weak (↔Sox9) and/or non-specific (↑TNAP; Figure 1). In contrast, the "Bone" scaffold formulation was associated with a clear osteogenic response relative to "PEG" controls (↑TNAP, ↑OPN, ↑mineralization, with ↔Sox9 and ↔Col II; Figure 1) While we did not control for donor variability in all of our scaffold development studies due to practical reasons, we observed minimal effect of donor with our osteogenic scaffolds (Supporting Information Figure S4), as was observed previously for bone marrow derived MSCs.[43]

The relatively weak SMSC chondrogenic response to PEG-HA_{IMW}-TGFβ1 scaffolds led us to further investigate the "Cartilage" scaffold. Unfortunately, co-culturing PEG-HA_{IMW}-TGFβ1 and PEG-PDMS-BMP2 constructs yielded no improvement with respect to chondrogenesis, and generally had an osteogenic effect on the "Cartilage" constructs (↓Sox9, ↑OPN) without influencing SMSCs cultured in "Bone" scaffolds (Figures 2 and 3). Thus, we revised our initial 'Cartilage' formulation, substituting HA_{IMW} with CSC. Similar to HA_{IMW}, CSC is a GAG component of native cartilage ECM that is widely utilized in cartilage bioengineering applications.[58,96] Interestingly, incorporation of CSC into our PEGDA networks stimulated an enhanced SMSC chondrogenic response relative to HA_{IMW} (↑Sox9, ↑aggrecan, ↓TNAP; Figure 4). Our results compare favorably with previous work demonstrating enhanced bone marrow MSC chondrogenesis (↑Col II:Col X and ↑Sox9 mRNA) in scaffolds containing CSC compared to HA.[66,97] Given that the bulk compressive modulus was similar across our scaffold formulations (Supporting Information Table S1), the enhanced chondrogenic response observed in PEG-CSC-TGFβ1 versus PEG-HA_{IMW}−TGFβ1 scaffolds may be due to complex, differential cell-ECM, growth factor-ECM, and ion-ECM interactions mediated by anionic GAG domains.[98,99]

After refining the "Cartilage" formulation to support more robust chondrogenesis, a "Transition" scaffold was fabricated to contain a graded mixture of the chondrogenic and osteogenic signals utilized in the PEG-CSC-TGFβ1 "Cartilage" constructs and the PEG-PDMS-BMP2 "Bone" constructs. This "Transition" scaffold was intended to promote SMSCs to take on a hypertrophic chondrocytic phenotype mimetic of the osteochondral "transition zone" at the cartilage-bone interface. The effects of the "Cartilage," "Transition," and "Bone" constructs on SMSCs were then compared. As anticipated, SMSCs within the 'Cartilage' formulation exhibited a phenotypic signature most aligned with non-hypertrophic chondrocytic behavior (↑Sox9, ↑Col II, ↓Col X, ↓TNAP, ↓OPN, and ↓mineralization) of the zonal formulations. These results are consistent with the incorporation of CSC into PEG-networks, which has been shown to induce stable chondrogenesis in MSCs and prevent hypertrophic differentiation.[39,65]

Aside from the general trends observed between "Cartilage" and the other two zones, more subtle differences between phenotypes were also present between "Transition" and "Bone." For example, the "Transition" and "Bone" constructs had similar levels of mineralization but differed in other aspects of their phenotypic profile. Specifically, "Transition" scaffolds stimulated the highest levels of the hypertrophic marker Col X of the formulations examined (Figure 5). Similarly, the "Bone" scaffolds—which contained the highest levels of osteoinductive PDMS and BMP2—induced the greatest expression of osteogenic markers

Author Manuscript Author Manuscript Author Manuscript Author Manuscript

TNAP and OPN, in agreement with previous bone marrow MSC studies.[43] Overall, these results suggest that a graded transition from PEG-CSC-TGFβ1 to PEG-PDMS-BMP2 scaffolds elicits a gradual SMSC phenotypic shift from chondrocyte to hypertrophic chondrocyte to osteoblast-like. As such, further development of these scaffold formulations for use in SMSC-based OCD repair is warranted.

Several limitations of the present study merit comment. First, extrapolating our findings to humans is not guaranteed due to the experimental system utilized (*in vitro* culture with canine SMSCs). We evaluated canine SMSC responses rather than human cells in this initial study because OCD treatments must demonstrate efficacy in large animal preclinical studies before advancing to humans, and canine *in vivo* models of OCD defects offer several advantages over other large animals. Indeed, the overall degree of similarity between human and canine with respect to bone composition,[100] cell and tissue response to stimuli,[101–109] and pathological outcomes[110–113] highlights a significant overlap in behaviors. Second, although we identified scaffold formulations which independently favored zonally-specific SMSC behavior, implementing these formulations as a scaffold for OCD repair will require layer assembly and knowledge of how these constructs behave when placed in culture together. Moreover, future refinement of the zonal scaffold formulations may manipulate scaffold modulus in addition to biochemical cues to further promote induction of desired SMSC differentiation due to chondrogenesis and osteogenesis being favored at moduli between ~40 and 100 kPa.[114–118] However, incorporating these mechanical cues into a practical OCD construct may require a balance between this important mechanobiology variable and the load bearing nature of the osteochondral unit.

CONCLUSIONS

The present study investigated SMSC responses to PEG-based scaffold formulations with varying levels of chondrogenic and osteogenic cues. Overall, our results suggest that a graded transition from PEG-CSC-TGFβ1 to PEG-PDMS-BMP2 scaffolds elicits a desired SMSC phenotypic shift from chondrocyte to hypertrophic chondrocyte to osteoblast-like. Future work into the development of these scaffolds is both warranted and needed to achieve our long-term goal: the development of a PEG-based, zonally-tailored scaffold capable of guiding SMSC-based OCD repair. More broadly, the current study also supports the use of SMSCs for osteochondral tissue regeneration strategies, potentially overcoming current limitations associated with the harvest of bone marrow MSCs.

Supplementary Material

Refer to Web version on PubMed Central for supplementary material.

Acknowledgments

Contract grant sponsor: American Kennel Club Canine Health Foundation; contract grant number: 02078

Contract grant sponsor: National Institutes of Health; contract grant number: R01 DE025886R03 EB015202-01

Author Manuscript Author Manuscript Author Manuscript Author Manuscript

REFERENCES

1. Huey DJ, Hu JC, Athanasiou KA. Unlike bone, cartilage regeneration remains elusive. Science 2012;338(6109):917–921. [PubMed: 23161992]
2. Rodrigues MT, Gomes ME, Reis RL. Current strategies for osteochondral regeneration: from stem cells to pre-clinical approaches. Curr Opin Biotechnol 2011;22(5):726–733. [PubMed: 21550794]
3. Angel MJ, Razzano P, Grande DA. Defining the challenge – the basic science of articular cartilage repair and response to injury. Sports Med Arthroscopy Rev 2003;11:168–181.
4. Hjelle K, Solheim E, Strand T, Muri R, Brittberg M. Articular cartilage defects in 1,000 knee arthroscopies. Art Ther 2002;18: 730–734.
5. O' Driscoll SW. The healing and regeneration of articular cartilage. J Bone Joint Surg Am 1998;80:1795–1812. [PubMed: 9875939]
6. Bhosale AM, Richardson JB. Articular cartilage: structure, injuries and review of management. Br Med Bull 2008;87:77–95. [PubMed: 18676397]
7. Nukavarapu SP, Dorcemus DL. Osteochondral tissue engineering: current strategies and challenges. Biotechnol Adv 2013;31(5): 706–721. [PubMed: 23174560]
8. Yang PJ, Temenoff JS. Engineering orthopedic tissue interfaces. Tissue Eng B Rev 2009;15(2):127–141.
9. Lopa S, Madry H. Bioinspired scaffolds for osteochondral regeneration. Tissue Eng A 2014;20(15–16):2052–2076.
10. Ng J, Bernhard J, Vunjak-Novakovic G. Mesenchymal stem cells for osteochondral tissue engineering. Methods Mol Biol 2016; 1416:35–54. [PubMed: 27236665]
11. Jones BA, Pei M. Synovium-derived stem cells: a tissue-specific stem cell for cartilage engineering and regeneration. Tissue Eng B Rev 2012;18(4):301–311.
12. Kang BJ, Ryu HH, Park SS, Koyama Y, Kikuchi M, Woo HM, Kim WH, Kweon OK. Comparing the osteogenic potential of canine mesenchymal stem cells derived from adipose tissues, bone marrow, umbilical cord blood, and Wharton's jelly for treating bone defects. J Vet Sci 2012;13(3): 299–310. [PubMed: 23000587]
13. De Bari C, Dell'Accio F, Tylzanowski P, Luyten FP. Multipotent Mesenchymal stem cells from adult human synovial membrane. Arthritis Rheum 2001;44(8):1928–1942. [PubMed: 11508446]
14. Bearden RN, Huggins SS, Cummings KJ, Smith R, Gregory CA, Saunders WB. In-vitro characterization of canine multipotent stromal cells isolated from synovium, bone marrow, and adipose tissue: a donor-matched comparative study. Stem Cell Res Ther 2017;8:218. [PubMed: 28974260]
15. Fan J, Varshney RR, Ren L, Cai D, Wang DA. Synovium-derived Mesenchymal stem cells: a new cell source for musculoskeletal regeneration. Tissue Eng B Rev 2009;15(1):75–86.
16. Sakaguchi Y, Sekiya I, Yagishita K, Muneta T. Comparison of human stem cells derived from various mesenchymal tissues: superiority of synovium as a cell source. Arthritis Rheum 2005; 52(8):2521–2529. [PubMed: 16052568]
17. Lee S, Kim JH, Jo CH, Seong SC, Lee JC, Lee MC. Effect of serum and growth factors on Chondrogenic differentiation of Synovium-derived stromal cells. Tissue Eng A 2009;15(11):3401–3415.
18. Kim YI, Ryu JS, Yeo JE, Choi YJ, Kim YS, Ko K, Koh YG. Overexpression of TGF-beta 1 enhances chondrogenic differentiation and proliferation of human synovium-derived stem cells. Biochem Biophys Res Commun 2014;450(4):1593–1599. [PubMed: 25035928]
19. Pei M, He F, Vunjak-Novakovic G. Synovium-derived stem cell-based chondrogenesis. Differentiation 2008;76(10):1044–1056. [PubMed: 18637024]
20. Kurth T, Hedbom E, Shintani N, Sugimoto M, Chen FH, Haspl M, Martinovic S, Hunziker EB. Chondrogenic potential of human synovial mesenchymal stem cells in alginate. Osteoarthr Cartil 2007;15(10):1178–1189. [PubMed: 17502159]
21. Shields LBE, Raque GH, Glassman SD, Campbell M, Vitaz T, Harpring J, Shields CB. Adverse effects associated with high-dose recombinant human bone morphogenetic protein-2 use in anterior cervical spine fusion. Spine 2006;31(5):542–547. [PubMed: 16508549]

Author Manuscript Author Manuscript Author Manuscript Author Manuscript

22. Smucker JD, Rhee JM, Singh K, Yoon ST, Heller JG. Increased swelling complications associated with off-label usage of rhBMP-2 in the anterior cervical spine. Spine 2006;31(24):2813–2819. [PubMed: 17108835]

23. Fragiadaki M, Ikeda T, Witherden A, Mason RM, Abraham D, Bou-Gharios G. High doses of TGF-beta potently suppress type I collagen via the transcription factor CUX1.Mol Biol Cell 2011;22(11):1836–1844. [PubMed: 21471005]

24. Shimomura K, Ando W, Moriguchi Y, Sugita N, Yasui Y, Koizumi K, Fujie H, Hart DA, Yoshikawa H, Nakamura N. Next generation Mesenchymal stem cell (MSC)-based cartilage repair using scaffold-free tissue engineered constructs generated with synovial Mesenchymal stem cells. Cartilage 2015;6(2):13s–29s. [PubMed: 27340513]

25. Koizumi K, Ebina K, Hart DA, Hirao M, Noguchi T, Sugita N, Yasui Y, Chijimatsu R, Yoshikawa H, Nakamura N. Synovial mesenchymal stem cells from osteo-or rheumatoid arthritis joints exhibit good potential for cartilage repair using a scaffold-free tissue engineering approach. Osteoarthr Cartil 2016;24(8):1413–1422. [PubMed: 26973329]

26. Koga H, Muneta T, Nagase T, Nimura A, Ju YJ, Mochizuki T, Sekiya I. Comparison of mesenchymal tissues-derived stem cells for in vivo chondrogenesis: suitable conditions for cell therapy of cartilage defects in rabbit. Cell Tissue Res 2008;333(2):207–215. [PubMed: 18560897]

27. Pan JF, Yuan L, Guo CA, Geng XH, Fei T, Fan WS, Li S, Yuan HF, Yan ZQ, Mo XM. Fabrication of modified dextran-gelatin in situ forming hydrogel and application in cartilage tissue engineering. J Mater Chem B 2014;2(47):8346–8360.

28. Shimomura K, Moriguchi Y, Ando W, Nansai R, Fujie H, Hart DA, Gobbi A, Kita K, Horibe S, Shino K. Others. Osteochondral repair using a scaffold-free tissue-engineered construct derived from synovial Mesenchymal stem cells and a hydroxyapatite-based artificial bone. Tissue Eng A 2014;20(17–18):2291–2304.

29. Wang YJ, Shi XT, Ren L, Yao YC, Wang DA. In vitro Osteogenesis of Synovium Mesenchymal cells induced by controlled release of alendronate and dexamethasone from a sintered microspherical scaffold. J Biomater Sci Polymer Ed 2010;21(8–9):1227–1238.

30. Pan JF, Li S, Guo CA, Xu DL, Zhang F, Yan ZQ, Mo XM. Evaluation of synovium-derived mesenchymal stem cells and 3D printed nanocomposite scaffolds for tissue engineering. Sci Technol Adv Mater 2015;16(4):045001. [PubMed: 27877821]

31. Tu XL, Wang LN, Wei J, Wang B, Tang YD, Shi J, Zhang ZJ, Chen Y.3D printed printed PEGDA microstructures for gelatin scaffold integration and neuron differentiation. Microelectron Eng 2016;158:30–34.

32. Seo H, Heo SG, Lee H, Yoon H. Preparation of PEG materials for constructing complex structures by stereolithographic 3D printing. RSC Adv 2017;7(46):28684–28688.

33. Bailey BM, Nail LN, Grunlan MA. Continuous gradient scaffolds for rapid screening of cell-material interactions and interfacial tissue regeneration. Acta Biomater 2013;9(9):8254–8261. [PubMed: 23707502]

34. Burdick JA, Khademhosseini A, Langer R. Fabrication of gradient hydrogels using a microfluidics/photopolymerization process. Langmuir 2004;20(13):5153–5156. [PubMed: 15986641]

35. Chatterjee K, Lin-Gibson S, Wallace WE, Parekh SH, Lee YJ, Cicerone MT,Young MF, Simon CG. The effect of 3D hydrogel scaffold modulus on osteoblast differentiation and mineralization revealed by combinatorial screening. Biomaterials 2010;31(19):5051–5062. [PubMed: 20378163]

36. Hahn MS, Taite LJ, Moon JJ, Rowland MC, Ruffino KA, West JL. Photolithographic patterning of polyethylene glycol hydrogels. Biomaterials 2006;27(12):2519–2524. [PubMed: 16375965]

37. Gombotz WR, Guanghui W, Horbett TA, Hoffman AS. Protein adsorption to poly(ethylene oxide) surfaces. J Biomed Mater Res 1991;25(12):1547–1562. [PubMed: 1839026]

38. Munoz-Pinto DJ, Jimenez-Vergara AC, Gelves LM, McMahon RE, Guiza-Arguello V, Hahn MS. Probing vocal fold fibroblast response to hyaluronan in 3D contexts. Biotechnol Bio eng 2009;104(4): 821–831.

39. Varghese S, Hwang NS, Canver AC, Theprungsirikul P, Lin DW, Elisseeff J. Chondroitin sulfate based niches for chondrogenic differentiation of mesenchymal stem cells. Matrix Biol 2008;27(1): 12–21. [PubMed: 17689060]

Author Manuscript Author Manuscript Author Manuscript Author Manuscript

40. Mann BK, Schmedlen RH, West JL. Tethered-TGF-beta increases extracellular matrix production of vascular smooth muscle cells. Biomaterials 2001;22(5):439–444. [PubMed: 11214754]
41. Burdick JA, Mason MN, Hinman AD, Thorne K, Anseth KS. Delivery of osteoinductive growth factors from degradable PEG hydrogels influences osteoblast differentiation and mineralization. J Control Release 2002;83(1):53–63. [PubMed: 12220838]
42. Saik JE, Gould DJ, Watkins EM, Dickinson ME, West JL. Covalently immobilized platelet-derived growth factor-BB promotes angiogenesis in biomimetic poly(ethylene glycol) hydrogels. Acta Biomater 2011;7(1):133–143. [PubMed: 20801242]
43. Gharat TP, Diaz-Rodriguez P, Erndt-Marino JD, Jimenez Vergara AC, Munoz Pinto DJ, Bearden RN, Huggins SS, Grunlan M, Saunders WB, Hahn MS. A canine in vitro model for evaluation of marrow-derived mesenchymal stromal cell-based bone scaffolds. J Biomed Mater Res A 2018;106:2382–2393. [PubMed: 29633508]
44. DeLong SA, Moon JJ, West JL. Covalently immobilized gradients of bFGF on hydrogel scaffolds for directed cell migration. Biomaterials 2005;26(16):3227–3234. [PubMed: 15603817]
45. Williams CG, Kim TK, Taboas A, Malik A, Manson P, Elisseeff J. In vitro chondrogenesis of bone marrow-derived mesenchymal stem cells in a photopolymerizing hydrogel. Tissue Eng 2003;9(4): 679–688. [PubMed: 13678446]
46. Erndt-Marino J, Trinkle E, Hahn MS. Hyperosmolar potassium (K(+)) treatment suppresses osteoarthritic chondrocyte catabolic and inflammatory protein production in a 3-dimensional in vitro model. Cartilage 2017;1–10.
47. Bahney CS, Hsu CW, Yoo JU, West JL, Johnstone B. A bioresponsive hydrogel tuned to chondrogenesis of human mesenchymal stem cells. FASEB J 2011;25(5):1486–1496. [PubMed: 21282205]
48. Nguyen QT, Hwang Y, Chen AC, Varghese S, Sah RL. Cartilage-like mechanical properties of poly (ethylene glycol)-diacrylate hydrogels. Biomaterials 2012;33(28):6682–6690. [PubMed: 22749448]
49. Lin S, Sangaj N, Razafiarison T, Zhang C, Varghese S. Influence of physical properties of biomaterials on cellular behavior. Pharm Res 2011;28(6):1422–1430. [PubMed: 21331474]
50. Samavedi S, Diaz-Rodriguez P, Erndt-Marino JD, Hahn MS. A three-dimensional chondrocyte-macrophage coculture system to probe inflammation in experimental osteoarthritis. Tissue Eng A 2017;23(3–4):101–114.
51. Nuttelman CR, Benoit DS, Tripodi MC, Anseth KS. The effect of ethylene glycol methacrylate phosphate in PEG hydrogels on mineralization and viability of encapsulated hMSCs. Biomaterials 2006;27(8):1377–1386. [PubMed: 16139351]
52. Burdick JA, Anseth KS. Photoencapsulation of osteoblasts in injectable RGD-modified PEG hydrogels for bone tissue engineering. Biomaterials 2002;23(22):4315–4323. [PubMed: 12219821]
53. Erndt-Marino JD, Hahn MS. Probing the response of human osteoblasts following exposure to sympathetic neuron-like PC-12 cells in a 3D coculture model. J Biomed Mater Res A 2017;105(4): 984–990. [PubMed: 27860234]
54. McCall JD, Luoma JE, Anseth KS. Covalently tethered transforming growth factor beta in PEG hydrogels promotes chondrogenic differentiation of encapsulated human mesenchymal stem cells. Drug Deliv Transl Res 2012;2(5):305–312. [PubMed: 23019539]
55. Re'em T, Kaminer-Israeli Y, Ruvinov E, Cohen S. Chondrogenesis of hMSC in affinity-bound TGF-beta scaffolds. Biomaterials 2012; 33(3):751–761. [PubMed: 22019120]
56. Chung C, Burdick JA. Influence of three-dimensional hyaluronic acid microenvironments on Mesenchymal stem cell Chondrogenesis. Tissue Eng Part A 2009;15(2):243–254. [PubMed: 19193129]
57. Pfeifer CG, Berner A, Koch M, Krutsch W, Kujat R, Angele P, Nerlich M, Zellner J. Higher ratios of hyaluronic acid enhance chondrogenic differentiation of human MSCs in a hyaluronic acid-gelatin composite scaffold. Materials 2016;9(5):381.
58. Steinmetz NJ, Bryant SJ. Chondroitin sulfate and dynamic loading alter chondrogenesis of human MSCs in PEG hydrogels. Biotechnol Bio eng 2012;109(10):2671–2682.

Author Manuscript Author Manuscript Author Manuscript Author Manuscript

59. Munoz-Pinto DJ, Jimenez-Vergara AC, Hou Y, Hayenga HN, Rivas A, Grunlan M, Hahn MS. Osteogenic potential of poly(ethylene glycol)-poly(dimethylsiloxane) hybrid hydrogels. Tissue Eng Part A 2012;18(15–16):1710–1719. [PubMed: 22519299]
60. Hou Y, Schoener CA, Regan KR, Munoz-Pinto D, Hahn MS, Grunlan MA. Photo-cross-linked PDMSstar-PEG hydrogels: synthesis, characterization, and potential application for tissue engineering scaffolds. Biomacromolecules 2010;11(3):648–656. [PubMed: 20146518]
61. Munoz-Pinto DJ, McMahon RE, Kanzelberger MA, Jimenez-Vergara AC, Grunlan MA, Hahn MS. Inorganic-organic hybrid scaffolds for osteochondral regeneration. J Biomed Mater Res A 2010; 94(1):112–121. [PubMed: 20128006]
62. Bailey BM, Fei R, Munoz-Pinto D, Hahn MS, Grunlan MA. PDMS(star)-PEG hydrogels prepared via solvent-induced phase separation (SIPS) and their potential utility as tissue engineering scaffolds. Acta Biomater 2012;8(12):4324–4333. [PubMed: 22842033]
63. Ingavle GC, Dormer NH, Gehrke SH, Detamore MS. Using chondroitin sulfate to improve the viability and biosynthesis of chondrocytes encapsulated in interpenetrating network (IPN) hydrogels of agarose and poly(ethylene glycol) diacrylate. J Mater Sci Mater Med 2012;23(1): 157–170. [PubMed: 22116661]
64. Qu X, Jimenez-Vergara AC, Munoz-Pinto DJ, Ortiz D, McMahon RE, Cristancho D, Becerra-Bayona S, Guiza-Arguello V, Grande-Allen KJ, Hahn MS. Regulation of smooth muscle cell phenotype by glycosaminoglycan identity. Acta Biomater 2011;7(3): 1031–1039. [PubMed: 21094702]
65. Villanueva I, Gladem SK, Kessler J, Bryant SJ. Dynamic loading stimulates chondrocyte biosynthesis when encapsulated in charged hydrogels prepared from poly(ethylene glycol) and chondroitin sulfate. Matrix Biol 2010;29(1):51–62. [PubMed: 19720146]
66. Costantini M, Idaszek J, Szoke K, Jaroszewicz J, Dentini M, Barbetta A, Brinchmann JE, Swieszkowski W. 3D bioprinting of BM-MSCs-loaded ECM biomimetic hydrogels for in vitro neocartilage formation. Biofabrication 2016;8(3):035002. [PubMed: 27431574]
67. Kudo T, Nakatani S, Kakizaki M, Arai A, Ishida K, Wada M, Kobata K. Supplemented chondroitin sulfate and hyaluronic acid suppress mineralization of the Chondrogenic cell line, ATDC5, via direct inhibition of alkaline phosphatase. Biol Pharm Bull 2017; 40(12):2075–2080. [PubMed: 29199232]
68. Amann E, Wolff P, Breel E, van Griensven M, Balmayor ER. Hyaluronic acid facilitates chondrogenesis and matrix deposition of human adipose derived mesenchymal stem cells and human chondrocytes co-cultures. Acta Biomater 2017;52:130–144. [PubMed: 28131943]
69. Radhakrishnan J, Subramanian A, Sethuraman S. Injectable glycosaminoglycan-protein nano-complex in semi-interpenetrating networks: a biphasic hydrogel for hyaline cartilage regeneration. Carbohydr Polym 2017;175:63–74. [PubMed: 28917911]
70. Corradetti B, Taraballi F, Minardi S, Van Eps J, Cabrera F, Francis LW, Gazze SA, Ferrari M, Weiner BK, Tasciotti E. Chondroitin sulfate immobilized on a biomimetic scaffold modulates inflammation while driving Chondrogenesis. Stem Cells Transl Med 2016;5(5):670–682. [PubMed: 27013739]
71. Masters KS, Shah DN, Leinwand LA, Anseth KS. Crosslinked hyaluronan scaffolds as a biologically active carrier for valvular interstitial cells. Biomaterials 2005;26(15):2517–2525. [PubMed: 15585254]
72. Jimenez-Vergara AC, Munoz-Pinto DJ, Becerra-Bayona S, Wang B, Iacob A, Hahn MS. Influence of glycosaminoglycan identity on vocal fold fibroblast behavior. Acta Biomater 2011;7(11):3964–3972. [PubMed: 21740987]
73. Bauer C, Niculescu-Morzsa E, Jeyakumar V, Kern D, Spath SS, Nehrer S. Chondroprotective effect of high-molecular-weight hyaluronic acid on osteoarthritic chondrocytes in a co-cultivation inflammation model with M1 macrophages. J Inflam Lond 2016;13:31.
74. Hahn MS, Miller JS, West JL. Laser scanning lithography for surface micropatterning on hydrogels. Adv Mater 2005;17(24): 2939–2942.
75. Hahn MS, Miller JS, West JL. Three-dimensional biochemical and biomechanical patterning of hydrogels for guiding cell behavior. Adv Mater 2006;18(20):2679–2684.

Author Manuscript Author Manuscript Author Manuscript Author Manuscript

76. Ceuninck F, Pastoureau P, Sabatini M. Cartilage and osteoarthritis: volume 2: structure and in vivo analysis. Humana Press Incorporated; Totowa, New Jersey 2004.
77. Liu HW, Chen CH, Tsai CL, Lin IH, Hsiue GH. Heterobifunctional poly(ethylene glycol)-tethered bone morphogenetic protein-2-stimulated bone marrow mesenchymal stromal cell differentiation and osteogenesis. Tissue Eng 2007;13(5):1113–1124. [PubMed: 17355208]
78. He X, Liu Y, Yuan X, Lu L. Enhanced healing of rat calvarial defects with MSCs loaded on BMP-2 releasing chitosan/alginate/hydroxyapatite scaffolds. PLoS One 2014;9(8):e104061. [PubMed: 25084008]
79. Liu HW, Chen CH, Tsai CL, Hsiue GH. Targeted delivery system for juxtacrine signaling growth factor based on rhBMP-2-mediated carrier-protein conjugation. Bone 2006;39(4):825–836. [PubMed: 16782421]
80. Moeinzadeh S, Barati D, He X, Jabbari E. Gelation characteristics and osteogenic differentiation of stromal cells in inert hydrolytically degradable micellar polyethylene glycol hydrogels. Biomacromolecules 2012;13(7):2073–2086. [PubMed: 22642902]
81. Bryant SJ, Anseth KS. Hydrogel properties influence ECM production by chondrocytes photoencapsulated in poly(ethylene glycol) hydrogels. J Biomed Mater Res 2002;59(1):63–72. [PubMed: 11745538]
82. Buxton AN, Zhu J, Marchant R, West JL, Yoo JU, Johnstone B. Design and characterization of poly(ethylene glycol) photopolymerizable semi-interpenetrating networks for chondrogenesis of human mesenchymal stem cells. Tissue Eng 2007;13(10): 2549–2560. [PubMed: 17655489]
83. Nicodemus GD, Bryant SJ. The role of hydrogel structure and dynamic loading on chondrocyte gene expression and matrix formation. J Biomech 2008;41(7):1528–1536. [PubMed: 18417139]
84. Nicodemus GD, Skaalure SC, Bryant SJ. Gel structure has an impact on pericellular and extracellular matrix deposition, which subsequently alters metabolic activities in chondrocyte-laden PEG hydrogels. Acta Biomater 2011;7(2):492–504. [PubMed: 20804868]
85. Erndt-Marino JD, Munoz-Pinto DJ, Samavedi S, Jimenez-Vergara AC, Diaz-Rodriguez P, Woodard L, Zhang DW, Grunlan MA, Hahn MS. Evaluation of the osteoinductive capacity of polydopamine-coated poly(epsilon-caprolactone) diacrylate shape memory foams. ACS Biomater Sci Eng 2015;1(12):1220–1230.
86. Salinas CN, Anseth KS. The influence of the RGD peptide motif and its contextual presentation in PEG gels on human mesenchymal stem cell viability. J Tissue Eng Regen Med 2008;2(5):296–304. [PubMed: 18512265]
87. Benoit DSW, Schwartz MP, Durney AR, Anseth KS. Small functional groups for controlled differentiation of hydrogel-encapsulated human mesenchymal stem cells. Nat Mater 2008;7(10): 816–823. [PubMed: 18724374]
88. Salinas CN, Anseth KS. The enhancement of chondrogenic differentiation of human mesenchymal stem cells by enzymatically regulated RGD functionalities. Biomaterials 2008;29(15):2370–2377. [PubMed: 18295878]
89. Findlay DM, Kuliwaba JS. Bone-cartilage crosstalk: a conversation for understanding osteoarthritis. Bone Res 2016;4:16028. [PubMed: 27672480]
90. Olivotto E, Vitellozzi R, Fernandez P, Falcieri E, Battistelli M, Burattini S, Facchini A, Flamigni F, Santi S, Facchini A. et al. Chondrocyte hypertrophy and apoptosis induced by GRO alpha require three-dimensional interaction with the extracellular matrix and a co-receptor role of chondroitin sulfate and are associated with the mitochondrial splicing variant of cathepsin B. J Cell Physiol 2007;210(2):417–427. [PubMed: 17096385]
91. Shibata S, Suda N, Suzuki S, Fukuoka H, Yamashita Y. An in situ hybridization study of Runx2, Osterix, and Sox9 at the onset of condylar cartilage formation in fetal mouse mandible. J Anat 2006;208(2):169–177. [PubMed: 16441561]
92. Cheng SH, Xing WR, Zhou X, Mohan S. Haploinsufficiency of osterix in chondrocytes impairs skeletal growth in mice. Physiol Genom 2013;45(19):917–923.
93. Dy P, Wang WH, Bhattaram P, Wang QQ, Wang L, Ballock RT, Lefebvre V. Sox9 directs hypertrophic maturation and blocks osteoblast differentiation of growth plate chondrocytes. Dev Cell 2012; 22(3):597–609. [PubMed: 22421045]

Author Manuscript Author Manuscript Author Manuscript Author Manuscript

94. McMahon LA, O'Brien FJ, Prendergast PJ. Biomechanics and mechanobiology in osteochondral tissues. Regen Med 2008;3(5): 743–759. [PubMed: 18729798]
95. Panseri S, Russo A, Cunha C, Bondi A, Di Martino A, Patella S, Kon E. Osteochondral tissue engineering approaches for articular cartilage and subchondral bone regeneration. Knee Surg Sports Traumatol Arthrosc 2012;20(6):1182–1191. [PubMed: 21910001]
96. Wang DA, Varghese S, Sharma B, Strehin I, Fermanian S, Gorham J, Fairbrother DH, Cascio B, Elisseeff JH. Multifunctional chondroitin sulphate for cartilage tissue-biomaterial integration. Nat Mater 2007;6(5):385–392. [PubMed: 17435762]
97. Matsiko A, Levingstone TJ, O'Brien FJ, Gleeson JP. Addition of hyaluronic acid improves cellular infiltration and promotes earlystage chondrogenesis in a collagen-based scaffold for cartilage tissue engineering. J Mech Behav Biomed Mater 2012;11:41–52. [PubMed: 22658153]
98. Gama CI, Tully SE, Sotogaku N, Clark PM, Rawat M, Vaidehi N, Goddard WA, Nishi A, Hsieh-Wilson LC. Sulfation patterns of glycosaminoglycans encode molecular recognition and activity. Nat Chem Biol 2006;2(9):467–473. [PubMed: 16878128]
99. Gao Y, Liu SY, Huang JX, Guo WM, Chen JF, Zhang L, Zhao B, Peng J, Wang AY, Wang Y. The ECM-cell interaction of cartilage extracellular matrix on chondrocytes. Biomed Res Int 2014;2014:1–8.
100. Aerssens J, Boonen S, Lowet G, Dequeker J. Interspecies differences in bone composition, density, and quality: potential implications for in vivo bone research. Endocrinology 1998;139(2): 663–670. [PubMed: 9449639]
101. Requicha JF, Viegas CA, Albuquerque CM, Azevedo JM, Reis RL, Gomes ME. Effect of anatomical origin and cell passage number on the stemness and osteogenic differentiation potential of canine adipose-derived stem cells. Stem Cell Rev 2012;8(4):1211–1222.
102. Garetto LP, Chen J, Parr JA, Roberts WE. Remodeling dynamics of bone supporting rigidly fixed titanium implants: a histomorphometric comparison in four species including humans. Implant Dent 1995;4(4):235–243. [PubMed: 8603133]
103. Au AY, Au RY, Demko JL, McLaughlin RM, Eves BE, Frondoza CG. Consil bioactive glass particles enhance osteoblast proliferation and selectively modulate cell signaling pathways in vitro. J Biomed Mater Res A 2010;94(2):380–388. [PubMed: 20186728]
104. Ding X, Zhou L, Wang J, Zhao Q, Lin X, Gao Y, Li S, Wu J, Rong M, Guo Z. The effects of hierarchical micro/nanosurfaces decorated with TiO2 nanotubes on the bioactivity of titanium implants in vitro and in vivo. Int J Nanomed 2015;10:6955–6973.
105. Kim MH, Park K, Choi KH, Kim SH, Kim SE, Jeong CM, Huh JB. Cell adhesion and in vivo osseointegration of sandblasted/acid etched/anodized dental implants. Int J Mol Sci 2015;16(5): 10324–10336. [PubMed: 25955650]
106. Kim SE, Kim CS, Yun YP, Yang DH, Park K, Kim SE, Jeong CM, Huh JB. Improving osteoblast functions and bone formation upon BMP-2 immobilization on titanium modified with heparin. Carbohydr Polym 2014;114:123–132. [PubMed: 25263872]
107. Wu X, Liu X, Wei J, Ma J, Deng F, Wei S. Nano-TiO2/PEEK bioactive composite as a bone substitute material: in vitro and in vivo studies. Int J Nanomed 2012;7:1215–1225.
108. Nie FL, Zheng YF, Wei SC, Wang DS, Yu ZT, Salimgareeva GK, Polyakov AV, Valiev RZ. In vitro and in vivo studies on nanocrystalline Ti fabricated by equal channel angular pressing with microcrystalline CP Ti as control. J Biomed Mater Res A 2013;101(6): 1694–1707. [PubMed: 23184756]
109. Im GI, Qureshi SA, Kenney J, Rubash HE, Shanbhag AS. Osteoblast proliferation and maturation by bisphosphonates. Biomaterials 2004;25(18):4105–4115. [PubMed: 15046901]
110. Morello E, Martano M, Buracco P. Biology, diagnosis and treatment of canine appendicular osteosarcoma: similarities and differences with human osteosarcoma. Vet J 2011;189(3):268–277. [PubMed: 20889358]
111. Paoloni M, Davis S, Lana S, Withrow S, Sangiorgi L, Picci P, Hewitt S, Triche T, Meltzer P, Khanna C. Canine tumor crossspecies genomics uncovers targets linked to osteosarcoma progression. BMC Genom 2009;10:625.
112. Sottnik JL, Campbell B, Mehra R, Behbahani-Nejad O, Hall CL, Keller ET. Osteocytes serve as a progenitor cell of osteosarcoma. J Cell Biochem 2014;115(8):1420–1429. [PubMed: 24700678]

Author Manuscript Author Manuscript Author Manuscript Author Manuscript

113. Fossey SL, Liao AT, McCleese JK, Bear MD, Lin J, Li PK, Kisseberth WC, London CA. Characterization of STAT3 activation and expression in canine and human osteosarcoma. BMC Cancer 2009;9:81. [PubMed: 19284568]

114. Parekh SH, Chatterjee K, Lin-Gibson S, Moore NM, Cicerone MT, Young MF, Simon CG. Modulus-driven differentiation of marrow stromal cells in 3D scaffolds that is independent of myosin-based cytoskeletal tension. Biomaterials 2011;32(9):2256–2264. [PubMed: 21176956]

115. Huebsch N, Arany PR, Mao AS, Shvartsman D, Ali OA, Bencherif SA, Rivera-Feliciano J, Mooney DJ. Harnessing tractionmediated manipulation of the cell/matrix interface to control stem-cell fate. Nat Mater 2010;9(6):518–526. [PubMed: 20418863]

116. Discher DE, Sweeney L, Sen S, Engler A. Matrix elasticity directs stem cell lineage specification. Biophys J 2007;126:32a–32a.

117. Lee J, Abdeen AA, Huang TH, Kilian KA. Controlling cell geometry on substrates of variable stiffness can tune the degree of osteogenesis in human mesenchymal stem cells. J Mech Behav Biomed Mater 2014;38:209–218. [PubMed: 24556045]

118. Park JS, Chu JS, Tsou AD, Diop R, Tang ZY, Wang AJ, Li S. The effect of matrix stiffness on the differentiation of mesenchymal stem cells inresponsetoTGF-beta. Biomaterials 2011;32(16): 3921–3930. [PubMed: 21397942]

Author Manuscript Author Manuscript Author Manuscript Author Manuscript

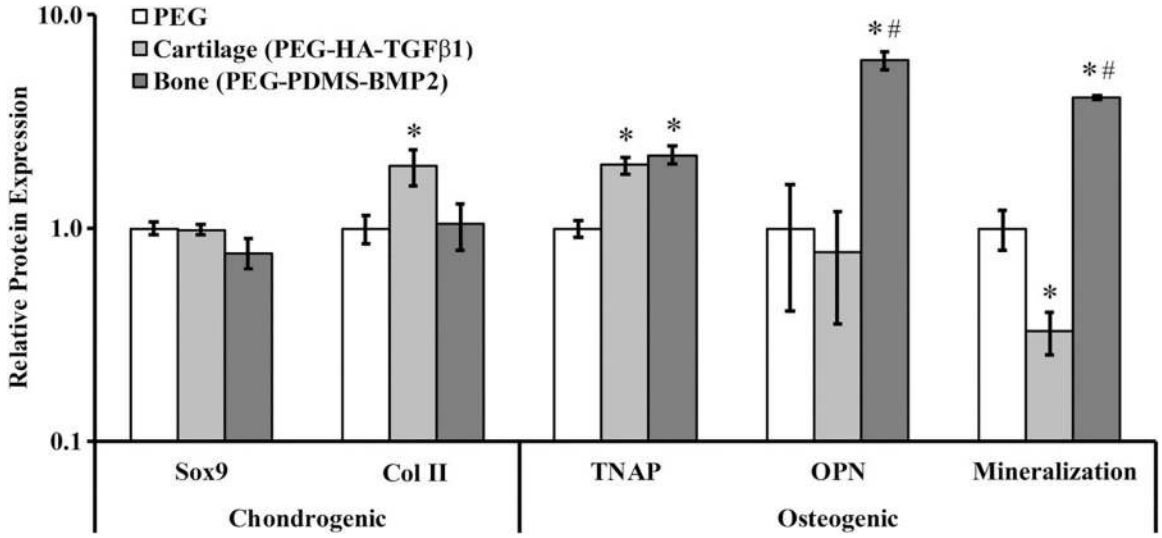

FIGURE 1.

Relative levels of chondrogenic markers Sox9 and Col II and osteogenic markers TNAP, OPN, and mineralization in SMSCs cultured in various scaffold formulations for 21 days. Data are presented relative to PEG scaffold controls. * denotes a significant difference relative to "PEG" scaffolds. # denotes a significant difference relative to "Cartilage" scaffolds. OPN, osteopontin; PEG, poly(ethylene) glycol; SMSCs, synovium-derived mesenchymal stem cells; TNAP, tissue non-specific alkaline phosphatase.

Author Manuscript Author Manuscript Author Manuscript Author Manuscript

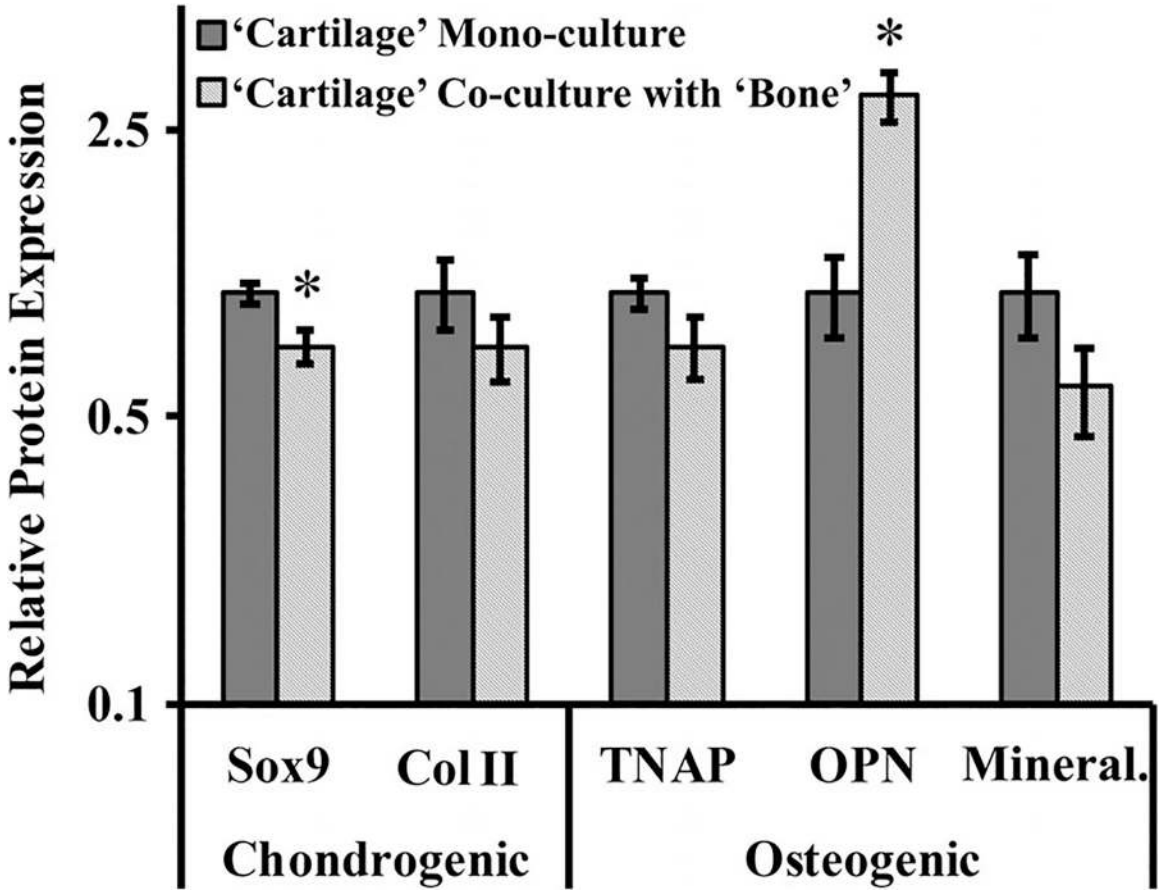

FIGURE 2.

Relative levels of chondrogenic markers Sox9 and Col II and osteogenic markers TNAP, OPN, and mineralization in SMSCs cultured in "Cartilage" constructs with or without co-culture with complementary "Bone" constructs for 21 days. Data are presented relative to the mono-culture experimental group. * denotes a significant difference relative to mono-culture. OPN, osteopontin; SMSCs, synovium-derived mesenchymal stem cells; TNAP, tissue non-specific alkaline phosphatase.

Author Manuscript Author Manuscript Author Manuscript Author Manuscript

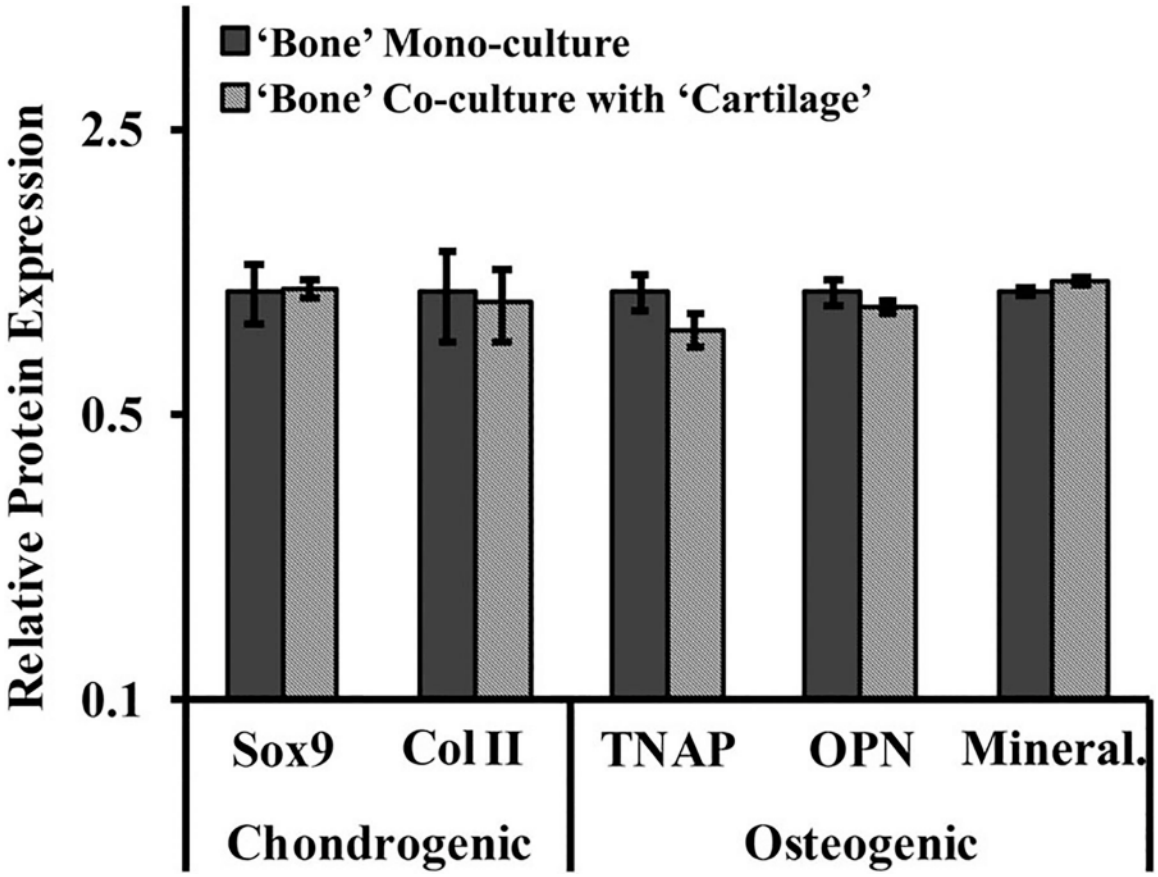

FIGURE 3.

Relative levels of chondrogenic markers Sox9 and Col II and osteogenic markers TNAP, OPN, and mineralization in SMSCs cultured in "Bone" constructs with or without co-culture with complementary "Cartilage" constructs for 21 days. Data are presented relative to the mono-culture experimental group. OPN, osteopontin; SMSCs, synovium-derived mesenchymal stem cells; TNAP, tissue non-specific alkaline phosphatase.

Author Manuscript Author Manuscript Author Manuscript Author Manuscript

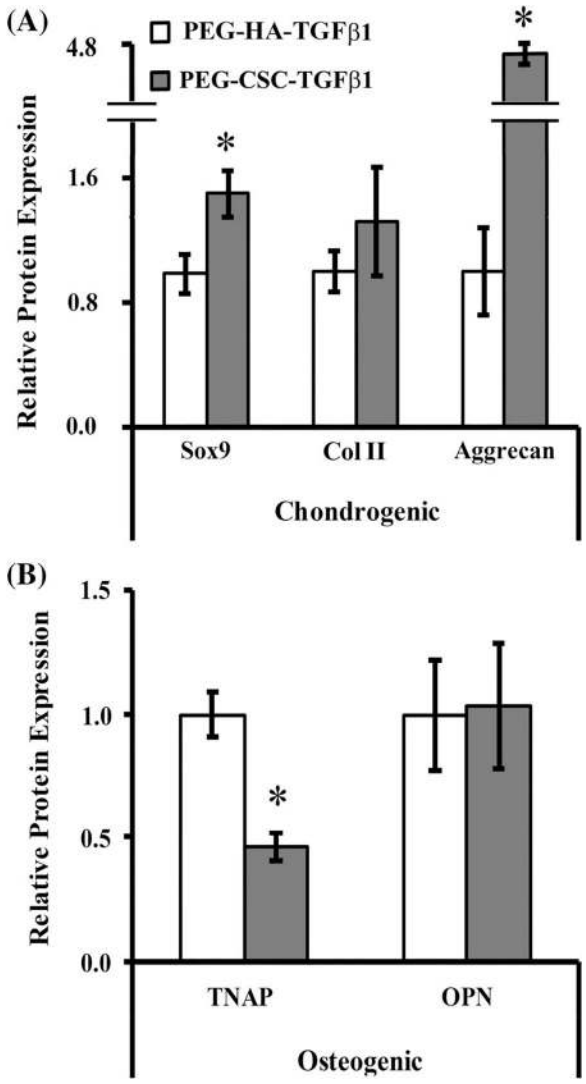

FIGURE 4.

Relative protein levels of (A) chondrogenic markers Sox9 and Col II and aggrecan (B) osteogenic markers TNAP and OPN in SMSCs cultured in either PEG-HA_{IMW}-TGFβ1 or PEG-CSC-TGFβ1 constructs for 21 days. Data are presented relative to the PEG-HA_{IMW}-TGFβ1 constructs. * denotes a significant difference relative to PEG-HA_{IMW}-TGFβ1. CSC, chondroitin-6-sulfate; HA, hyaluronan; OPN, osteopontin; PEG, poly(ethylene) glycol; SMSCs, synovium-derived mesenchymal stem cells; TGF, transforming growth factor; TNAP, tissue non-specific alkaline phosphatase.

Author Manuscript Author Manuscript Author Manuscript Author Manuscript

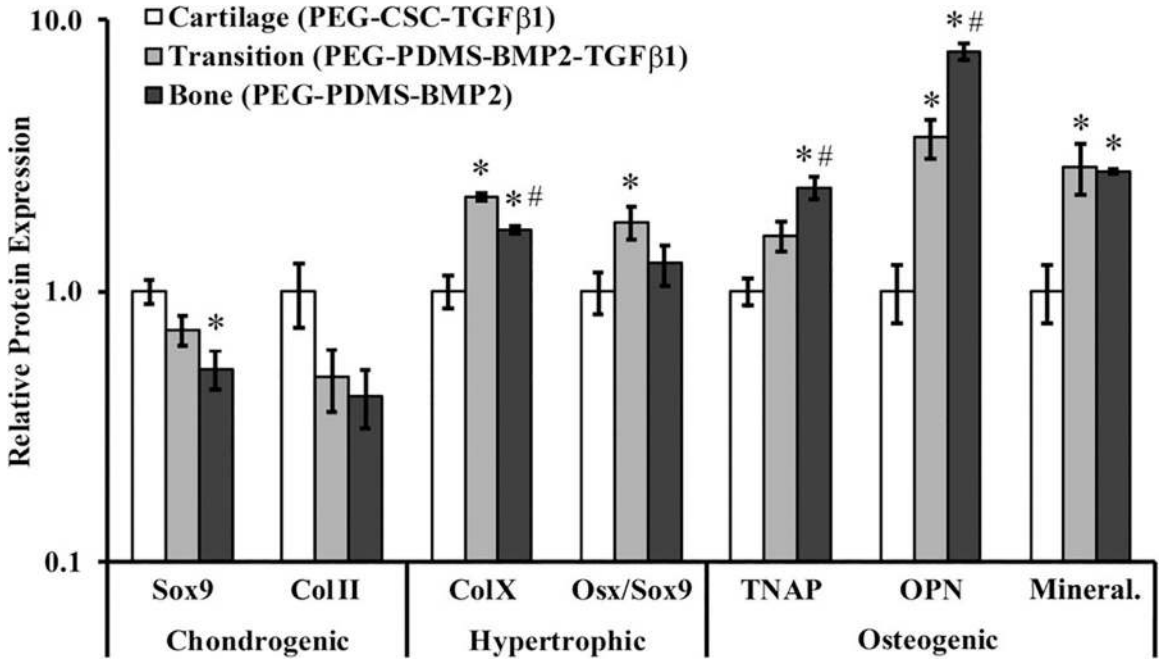

FIGURE 5.

Relative levels of chondrogenic markers Sox9 and Col II, hypertrophic markers Col X and Osx/Sox9, and osteogenic markers TNAP, OPN, and mineralization in SMSCs seeded in various scaffolds designed to elicit zonally-specific cell phenotypes. Data are presented relative to the "Cartilage" constructs. * denotes a significant difference relative to "Cartilage". # denotes a significant difference relative to "Transition". OPN, osteopontin; SMSCs, synovium-derived mesenchymal stem cells; TNAP, tissue non-specific alkaline phosphatase.